

## Irreversible mass loss of Canadian Arctic Archipelago glaciers

Jan T. M. Lenaerts,<sup>1</sup> Jan H. van Angelen,<sup>1</sup> Michiel R. van den Broeke,<sup>1</sup> Alex S. Gardner,<sup>2</sup> Bert Wouters,<sup>3</sup> and Erik van Meijgaard<sup>4</sup>

Received 14 December 2012; accepted 1 February 2013; published 7 March 2013.

[1] The Canadian Arctic Archipelago (CAA) contains the largest volume of glacier ice on Earth outside of Antarctica and Greenland. In the absence of significant calving, CAA glacier mass balance is governed by the difference between surface snow accumulation and meltwater runoff—surface mass balance. Here we use a coupled atmosphere/snow model to simulate present-day and 21st century CAA glacier surface mass balance. Through comparison with Gravity Recovery and Climate Experiment mass anomalies and in situ observations, we show that the model is capable of representing present-day CAA glacier mass loss, as well as the dynamics of the seasonal snow cover on the CAA tundra. Next, we force this model until 2100 with a moderate climate warming scenario (AR5 RCP4.5). We show that enhanced meltwater runoff from CAA glaciers is not sufficiently compensated by increased snowfall. Extrapolation of these results toward an AR5 multimodel ensemble results in sustained 21st century CAA glacier mass loss in the vast majority (>99%) of the ~7000 temperature realizations. **Citation:** Lenaerts, J. T. M., J. H. van Angelen, M. R. van den Broeke, A. S. Gardner, B. Wouters and E. van Meijgaard (2013), Irreversible mass loss of Canadian Arctic Archipelago glaciers, *Geophys. Res. Lett.*, 40, 870–874, doi:10.1002/grl.50214.

### 1. Introduction

[2] The Canadian Arctic Archipelago (CAA) consists of some 36,000 islands, of which  $\sim 146 \times 10^3$  km<sup>2</sup> ( $\sim 10\%$ ) is covered by glaciers (Figure 1). The CAA can be divided into a northern (NCAA) and southern (SCAA) region; the NCAA includes both large and small ice caps and ice fields, such as the Agassiz, Devon, and Muller Ice Caps and the Prince of Wales and Northern Ellesmere icefields ( $\sim 105 \times 10^3$  km<sup>2</sup>, Gardner *et al.* [2011]). The SCAA ( $\sim 41 \times 10^3$  km<sup>2</sup>) has two major ice caps (Barnes and Penny) on Baffin Island, and icefields and smaller glaciers on Bylot Island and along the eastern coast of Baffin Island [Gardner *et al.*, 2012].

All Supporting Information may be found in the online version of this article.

<sup>1</sup>Institute for Marine and Atmospheric Research Utrecht, Utrecht, The Netherlands.

<sup>2</sup>Graduate School of Geography, Clark University, Worcester, Massachusetts, USA.

<sup>3</sup>Cooperative Institute for Research in Environmental Sciences, Boulder, Colorado, USA.

<sup>4</sup>Royal Netherlands Meteorological Institute, De Bilt, The Netherlands.

Corresponding author: J. T. M. Lenaerts, Institute for Marine and Atmospheric Research Utrecht, Utrecht University, 5 Princetonplein, 3584 CC Utrecht, The Netherlands. (jtm.lenaerts@gmail.com)

©2013. American Geophysical Union. All Rights Reserved.  
0094-8276/13/10.1002/grl.50214

[3] Since 2000, near-surface (2 m) and upper-air temperatures (700 hPa) have increased by 1–2 K [Gardner *et al.*, 2011; Sharp *et al.*, 2011; Koerner, 2005; Gardner and Sharp, 2007]. In response, CAA glaciers experienced pronounced mass loss in the past decade, as evident from in situ surface mass balance (SMB) measurements [Gardner *et al.*, 2011; Sharp *et al.*, 2011; Zdanowicz *et al.*, 2012], laser altimetry [Gardner *et al.*, 2011, 2012], and stereoscopic imagery [Gardner *et al.*, 2012]. The Gravity Recovery and Climate Experiment twin satellites (GRACE) [Wouters *et al.*, 2008; Gardner *et al.*, 2011, 2012; Jacob *et al.*, 2012] detected a 2004–2011 CAA mass loss of  $579 \pm 33$  Gt. CAA glaciers lost mass at a rate of  $31 \pm 8$  Gt yr<sup>-1</sup> during 2004–2006, increasing to  $92 \pm 12$  Gt yr<sup>-1</sup> in the period 2007–2009 [Gardner *et al.*, 2011]. It has been unclear whether this sharp increase in mass loss was caused by natural decadal climate variability, or that it flagged the onset of a long-term decline of CAA glacier volume.

[4] Glacier mass balance ( $dM/dt$ ) equals the difference of SMB and solid ice discharge ( $D$ ). Mass loss through  $D$  in the CAA is small and is estimated at  $5 \pm 2$  Gt yr<sup>-1</sup> [Gardner *et al.*, 2011]. To date, no regionally complete observational estimate of  $D$  exists for either the NCAA or SCAA, and little is known about its temporal variability [Van Wychen *et al.*, 2012]. In this study, we therefore assume  $D$  to be constant in time, and CAA glacier mass balance to be governed by SMB, the difference between surface snow accumulation (precipitation minus evaporation) and meltwater runoff. Because in situ SMB measurements from CAA glaciers are scarce, high-resolution regional atmospheric climate models with detailed snow/ice melt physics are necessary to dynamically downscale atmospheric processes to assess past, present, and future CAA surface mass changes [Gready, 2012]. To date, modeling CAA glacier SMB has been based on empirical relations based on degree-days [Gardner *et al.*, 2011] or statistical downscaling of global models [Radić and Hock, 2011; Marzeion *et al.*, 2012], methods that are unable to resolve important atmosphere-surface feedback. In this study, we force a coupled atmosphere/snow model that is forced by ERA-40 and ERA-Interim atmospheric fields (1960–2011), which allows us to put recent CAA mass loss in a longer-term perspective. The model is evaluated using available in situ observations and GRACE mass anomalies. To estimate 21st century CAA SMB evolution, we force the model until 2100 with a midrange climate warming scenario (AR5 RCP4.5).

### 2. Methods

[5] Here we use the regional atmospheric climate model RACMO2, which is interactively coupled to a snow/firn/ice model that includes a snow albedo scheme based on prognostic snow grain size evolution (Kuipers Munneke *et al.* [2011], Supporting Information). To simulate contemporary

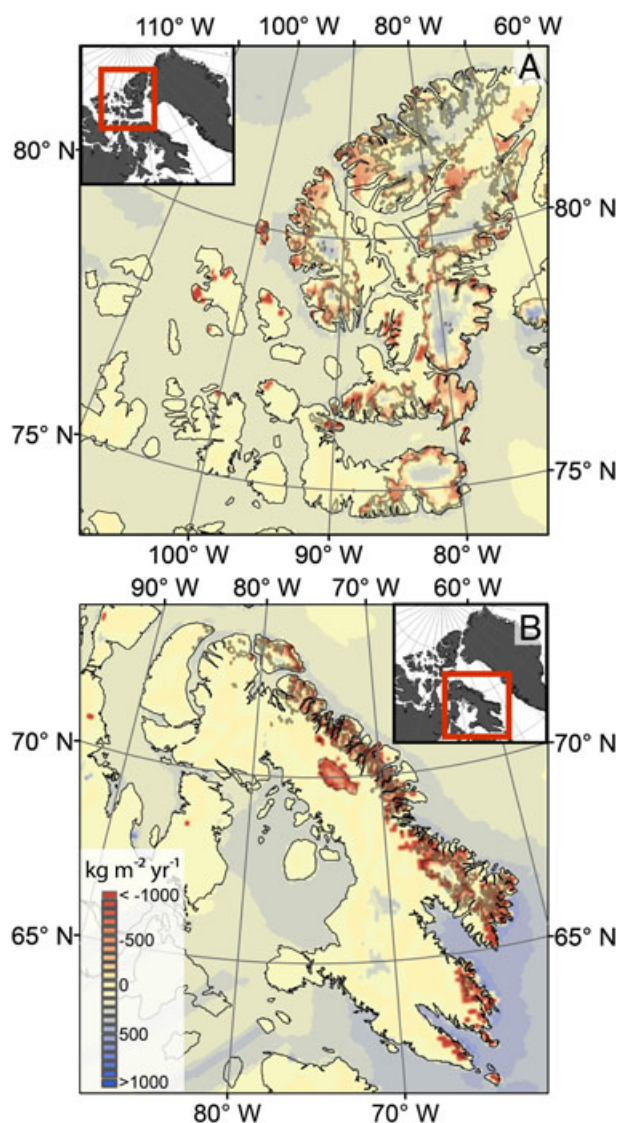


**Figure 1.** Mean modeled SMB (1960–2011) of the (A) NCAA and (B) SCAA and its vicinity. Note that SMB is only defined over glaciers (outlined by grey lines) and tundra, whereas over the ocean precipitation–evaporation is presented. The location of the regions is shown on the map inset in red.

climate, RACMO2 is forced by ERA-40 [Uppala *et al.*, 2005] and ERA-Interim [Dee *et al.*, 2011] global atmospheric reanalyses (1960–2011) and run at 11 km resolution, which is sufficient to resolve the hypsometry of most CAA glaciers (Figure S2). We applied an offline correction for the hypsometry bias in the model, which introduces a small SMB increase (see Supporting Information), but does not change the main conclusions of this study. RACMO2 realistically simulates annual precipitation (RMSE =  $134 \text{ kg m}^{-2} \text{ yr}^{-1}$ , Figure S1A) and near-surface temperature (RMSE =  $2.2 \text{ K}$ , Figure S1B). As a result, the spatial distribution of SMB (Figure 2A) and its temporal variability (Figure 2B) in RACMO2 compare very well with in situ SMB measurements. The model biases can be largely explained by elevation differences (inset Figure 2A), with the exception of Meighen Ice Cap (Supporting Information).

### 3. Results

#### 3.1. Recent CAA Glacier SMB

[6] During the past decade, CAA climate has been unfavorable for glaciers. The region is relatively dry, with typical precipitation rates of  $< 300 \text{ kg m}^{-2} \text{ yr}^{-1}$  in the northwest to  $> 500 \text{ kg m}^{-2} \text{ yr}^{-1}$  along the east-facing slopes surrounding Baffin Bay that experience enhanced orographic precipitation (Figure 1). Due to its high-Arctic location, the amplitude of the seasonal temperature cycle is large ( $30\text{--}50^\circ\text{C}$ ); in winter, the absence of solar radiation and the vicinity of the ice-covered Arctic Ocean enable very low near-surface temperatures ( $< -40^\circ\text{C}$ ). In contrast, summers are relatively mild, especially in SCAA ( $> 10^\circ\text{C}$ ), due to the proximity of snow-free land that efficiently absorbs solar radiation and the influence of warm continental air masses from the south [Gardner and Sharp, 2007].

[7] The rate and seasonality of CAA glacier mass loss in September 2003 to September 2012 (Figure 3) as measured by GRACE ( $69 \pm 6 \text{ Gt yr}^{-1}$ ) is well captured by RACMO2 ( $68 \pm 11 \text{ Gt yr}^{-1}$ ), but whereas mass losses in NCAA ( $37 \pm 10 \text{ Gt yr}^{-1}$ ) and SCAA ( $31 \pm 5 \text{ Gt yr}^{-1}$ ) are comparable in RACMO2, GRACE shows more mass loss in NCAA ( $46 \pm 5 \text{ Gt yr}^{-1}$ ) than in SCAA ( $23 \pm 3 \text{ Gt yr}^{-1}$ ). Part of these differences may be attributed to several issues that arise with the GRACE time series on subannual resolution, when applied to relatively small, partly glaciated areas. First, the signal includes a significant contribution from the growing and melting of the seasonal snow pack on the tundra surrounding the glaciers, artificially enhancing the seasonal cycle from  $95 \pm 24$  to  $217 \pm 42 \text{ Gt yr}^{-1}$ . In RACMO2 these effects can be separated (green and red lines in Figure 3), showing that a significant part of the seasonal cycle in GRACE derives from this effect. Second, the GRACE time series sometimes shows unphysical behavior, especially in periods of poor observational coverage.

[8] The overall good correspondence between RACMO2 and GRACE justifies a further exploration of processes responsible for CAA glacier mass loss. In the current climate, the SMB of CAA glaciers is primarily governed by precipitation, mostly snowfall, and meltwater runoff (Table S1). Modeled SMB decreases from  $-13 \pm 18 \text{ Gt yr}^{-1}$  in the period 1971–2000 to  $-51 \pm 26 \text{ Gt yr}^{-1}$  in 2000–2011, mainly as a result of a 54% increase in surface runoff ( $69$  to  $106 \text{ Gt yr}^{-1}$ ). Refreezing cannot (or only partly) compensate this mass loss, because warmer winters and high melt rates in spring quickly remove the cold content from the shallow winter snowpack. This implies that in the current climate, the CAA glacier snowpack has already reached its maximum refreezing capacity; in a warmer future climate, all additional meltwater will therefore run off without delay. 80% of the meltwater in CAA accumulation zone refreezes. That said, meltwater in the accumulation zone comprises a small fraction ( $< 20\%$ ) of the total and the potential for extra refreezing to buffer CAA mass loss is limited to  $2\text{--}3 \text{ Gt yr}^{-1}$ . This potential will only decrease with warming of the firm [Zdanowicz *et al.*, 2012] and shrinkage of accumulation area. Our model results indicate that the SMB of NCAA was near zero before 2000 (SMB =  $1 \pm 13 \text{ Gt yr}^{-1}$ ), which suggests that during the 20th century mass loss in the NCAA primarily occurred by calving. Surface mass loss set in after 2005 (SMB =  $-35 \pm 18 \text{ Gt yr}^{-1}$  during 2005–2011). In contrast, SCAA was already losing mass before 2000 (SMB =  $-15 \pm 11 \text{ Gt yr}^{-1}$  during

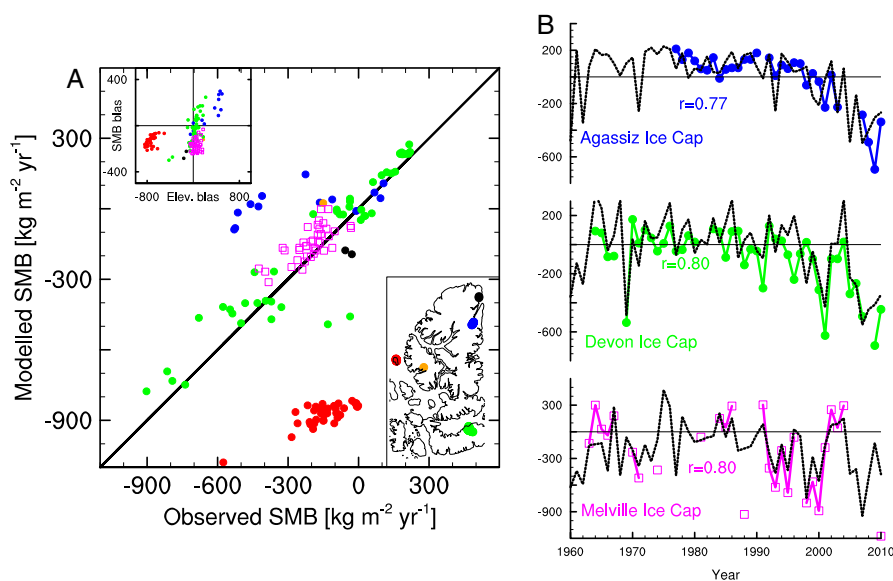


**Figure 2.** Modeled vs. observed SMB of NCAA glaciers. (A) The mean SMB for the period of the observational record (Supporting Information). The locations of the measurements are indicated in the lower inset. The purple squares represent measurements on Melville Ice Cap ( $75^{\circ}\text{N}$ ,  $115^{\circ}\text{W}$ ), which is located in western NCAA, but not shown on the inset map. The colored dots represent observations on Devon (green), Agassiz (blue), Meighen (red), Baby (orange), and Saint-Patrick (grey) ice caps. The upper inset shows SMB bias as a function of elevation bias. (B) Modeled (black) and observed (same colors as in A) time series of annual SMB ( $\text{kgm}^{-2} \text{yr}^{-1}$ ) for selected locations on Agassiz, Devon and Melville ice caps. At these locations, more than 20 years of SMB measurements are available. Measurements of consecutive years are connected by a colored line to show the interannual variability. Modeled SMB is from the grid point that is located nearest to the measurement site.

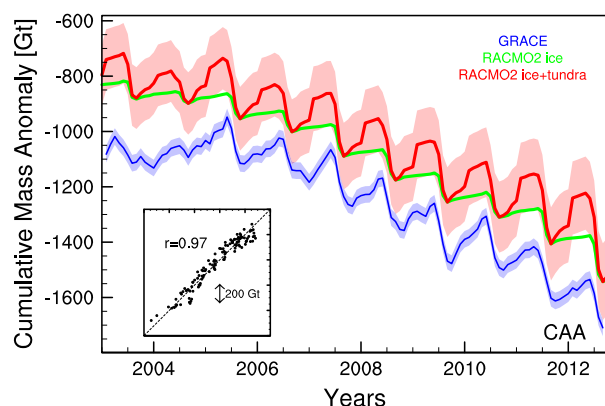


**Figure 3.** Recent (January 2003 to September 2012) cumulative mass anomalies in CAA from RACMO2 (land ice only in green and land ice plus seasonal snow on the tundra in red) and from GRACE (blue). The GRACE time series are offset by a fixed value to improve readability. RACMO2 mass anomalies include the calving estimates of  $5 \pm 2 \text{ Gt yr}^{-1}$  and are plotted with respect to the start of the simulation (January 1960). Related uncertainties are also shown in red for RACMO2 and in blue for GRACE. The correlation between RACMO2 (ice + tundra) and GRACE is shown in the inset. See Supporting Information for description of the methods and calculation of the uncertainties.

1971–2000), with mass loss in 2000–2011 increasing to  $-29 \pm 6 \text{ Gt yr}^{-1}$ . This finding is supported by recent mass balance estimates based on altimetry and stereographic imagery [Gardner *et al.*, 2012], showing a mass loss from

SCAA of  $-11 \pm 3 \text{ Gt yr}^{-1}$  between 1963 and 2006, increasing to  $-24 \pm 6 \text{ Gt yr}^{-1}$  in the period 2000–2011.

### 3.2. Persistent 21st Century Mass Loss

[9] To assess CAA mass loss for the remainder of the 21st century, RACMO2 was forced at the lateral boundaries with output from HadGEM2-ES [The HadGEM2 Development Team, 2011], a fully coupled Coupled Model Intercomparison Project Phase 5 (CMIP5) [Taylor *et al.*, 2007] general circulation model (GCM). The GCM in turn was forced with the modest warming scenario RCP4.5 [Moss *et al.*, 2010], resulting in a 21st century warming that is similar to the average of all Intergovernmental Panel on Climate Change (IPCC) AR5 multimodel scenarios (Supporting Information). In this GCM/scenario combination, global mean near-surface temperature increases by  $\sim 3.5 \text{ K}$  in 2080, and stabilizes afterward (Figure 4A). Twenty-first century warming in CAA is much stronger ( $\sim 8 \text{ K}$ ), owing to regional feedbacks such as the decreasing sea-ice cover, diminishing seasonal snow cover, and associated lowering of the surface albedo. When driven with these GCM output at its lateral boundaries, RACMO2 predicts significantly less warming in the CAA region,  $\sim 6.5 \text{ K}$  (Figure 4A), a result of the better resolved glacier ice cover and a more realistic snow model.

[10] Our results show that mean CAA glacier SMB decreases to  $-144 \pm 33 \text{ Gt yr}^{-1}$  at the end of the 21st century (Table S1). In contrast to the 20th century, mass loss is then larger in NCAA ( $\text{SMB} = -82 \pm 31 \text{ Gt yr}^{-1}$ ) than in SCAA ( $\text{SMB} = -62 \pm 10 \text{ Gt yr}^{-1}$ ). The mass loss is mainly caused by runoff, partly compensated by a  $\sim 30\%$  increase in precipitation (Figure 4B and Table S1). Total CAA surface mass loss represents 18% of its current volume by the end of the 21st century.

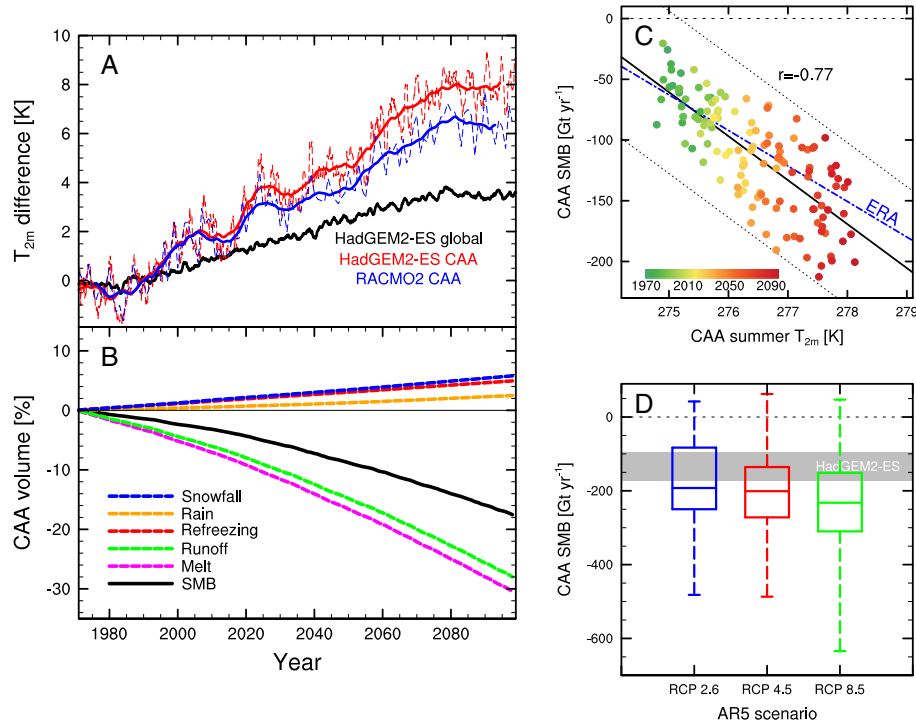


**Figure 4.** Results of HadGEM2-ES forced RACMO2 simulation (1971–2098). (A) Near-surface temperature; global (black) and CAA (red) from HadGEM2-ES directly, and CAA from RACMO2 driven by HadGEM2-ES (blue). Dashed lines are annual mean values; the solid lines are 20 year running averages. (B) Cumulative SMB and its components, plotted as a relative volume loss of CAA, taking the total volume of CAA to be  $80.16 \times 10^3 \text{ km}^3$  [Radić and Hock, 2011]. (C) Annual CAA SMB from RACMO2 as a function of mean summer (JJA) near-surface temperature according to HadGEM2-ES. The best linear fit ( $-36 \pm 3 \text{ Gt K}^{-1} \text{ yr}^{-1}$ ) is shown in black, whose slope compares well with that from the ERA reanalyses shown in blue (1960–2011,  $-29 \pm 4 \text{ Gt K}^{-1} \text{ yr}^{-1}$ ). The SMB uncertainty ( $67 \text{ Gt yr}^{-1}$ , Supporting Information) is indicated by the dotted lines. (D) Box plots of annual CAA SMB for all AR5 model results and all scenarios (2005–2098, see Supporting Information). The SMB uncertainty is included in the ensemble.  $\text{SMB} = 0$  is shown in Figures 4C and 4D as a dashed line.

[11] In spite of the warming ceasing, mass loss continues after 2080 (Figure 4B). The reason is that the glacier surface darkens: in the 21st century the mean surface albedo decreases by 4% as a result of lengthening of the melt season. Absorbed shortwave radiation, the main energy source of present-day melt, therefore continues to increase in the remainder of the 21st century (Figure S5). Other processes that enhance melt at the end of the 21st century are the absence of sea-ice in large parts of the Arctic Ocean (Figure S6), especially in summer and autumn, and a shorter duration of snow cover over the CAA tundra (10–40 days, Figure S6). At the end of the 21st century, snow cover in the SCAA becomes limited to the winter season (DJF), when albedo effects are small in the absence of sunlight.

[12] To assess the uncertainty of using a single GCM-scenario combination, we applied the significant linear relationship between CAA SMB and average summer (JJA) near-surface temperature in HadGEM2-ES (Figure 4C) to all ~7000 AR5 model CAA summer temperature scenarios for the 21st century (Supporting Information). Figure 4D confirms that the combination of HadGEM2-ES and the RCP4.5 emission scenario is relatively conservative. More importantly, CAA glacier growth ( $\text{SMB} > 0$ ) is predicted in less than 1% of the ensemble members, considering an SMB uncertainty of  $67 \text{ Gt yr}^{-1}$  (Supporting Information), which makes it highly unlikely that CAA glacier mass loss will reverse in the coming century. Considering the positive feedbacks and

reasonably assuming the atmospheric warming to continue in the coming two centuries, we believe that the mass loss is irreversible in the foreseeable future. Based on the full AR5-model ensemble, we estimate CAA glacier mass loss in the 21st century to be  $12,400 \pm 8,500 \text{ Gt}$ , equivalent to a eustatic sea level rise of  $0.35 \pm 0.24 \text{ mm yr}^{-1}$ . This is a conservative estimate, because our approach does not consider the positive feedback between surface lowering and melting (Supporting Information). It is nonetheless on the higher end of the recent estimate of  $0.27 \pm 0.12 \text{ mm yr}^{-1}$  [Radić and Hock, 2011] based on volume-area scaling and forced by the AR4 A1B scenario. Moreover, our estimates do not include the potential response of glacier dynamics to future warming, a process that is currently poorly constrained for the CAA and requires further study. Our results indicate that CAA will be the largest cryospheric contributor to 21st century sea level rise outside of Greenland and Antarctica [Radić and Hock, 2011; Rignot et al., 2011].

#### 4. Conclusions

[13] In this study, we used the coupled atmosphere/snow model RACMO2, evaluated with in situ observations, to simulate past, present, and future CAA glacier SMB. For the period before 2000, which marked the start of the recent trend of atmospheric warming, our results show distinct differences between NCAA, which was in approximate mass

balance, and SCAA, which was already clearly losing mass. From 2004 onward, RACMO2 indicates that CAA lost mass at a rate of  $64 \pm 10 \text{ Gt yr}^{-1}$ , which agrees well with GRACE ( $72 \pm 6 \text{ Gt yr}^{-1}$ ). Next, we forced RACMO2 with an AR5 GCM (HadGEM2-ES) and a moderate climate scenario (RCP 4.5). We found that the enhanced meltwater in the CAA snowpack does not refreeze and leads directly to increasing runoff. This increased meltwater runoff is only partly compensated by snowfall, and CAA SMB shows a decreasing trend throughout the century. We extrapolated the significant sensitivity of CAA SMB for summer near-surface temperature to all the  $\sim 7000$  AR5 temperature realizations. In nearly all projections ( $>99\%$ ), CAA SMB remains negative, suggesting persistent CAA mass loss throughout the remainder of the 21st century. Our results suggests a contribution of CAA glaciers to 21st century sea level rise of  $0.35 \pm 0.24 \text{ mm yr}^{-1}$ .

[14] **Acknowledgments.** We thank Geert Jan van Oldenborgh (Royal Netherlands Meteorological Institute) for making available the CMIP5 model data. This work was supported by funding from the ice2sea program from the European Union 7th Framework Programme, grant 226375. Ice2sea contribution number 110.

## References

- Dee, D. P., et al. (2011), The ERA-Interim reanalysis: Configuration and performance of the data assimilation system, *Quart. J. Roy. Meteor. Soc.*, *137*(656), 553–597, doi:10.1002/qj.828.
- Gardner, A. S., and M. Sharp (2007), Influence of the Arctic circumpolar vortex on the mass balance of Canadian high arctic glaciers, *J. Climate*, *20*(18), 4586–4598, doi:10.1175/JCLI4268.1.
- Gardner, A. S., G. Moholdt, B. Wouters, G. J. Wolken, D. O. Burgess, M. J. Sharp, J. G. Cogley, C. Braun, and C. Labine (2011), Sharply increased mass loss from glaciers and ice caps in the Canadian Arctic Archipelago, *Nature*, *473*, 357–360, doi:10.1038/nature10089.
- Gardner, A. S., G. Moholdt, A. Arendt, and B. Wouters (2012), Accelerated contributions of Canada's Baffin and Bylot Island glaciers to sea level rise over the past half century, *The Cryosphere*, *6*(5), 1103–1125, doi:10.5194/tc-6-1103-2012.
- Gready, B. P. (2012), Regional Climate Modeling over the Glaciated Regions of the Canadian High Arctic. PhD thesis, University of Alberta.
- Jacob, T., J. Wahr, W. T. Pfeffer, and S. Swenson (2012), Recent contributions of glaciers and ice caps to sea level rise, *Nature*, *482*, 514–518, doi:10.1038/nature10847.
- Koerner, R. M. (2005), Mass balance of glaciers in the Queen Elizabeth Islands, Nunavut, Canada, *Ann. Glaciol.*, *42*(1), 417–423, doi:10.3189/172756405781813122.
- Kuipers Munneke, P., M. R. van den Broeke, J. T. M. Lenaerts, M. G. Flanner, A. S. Gardner, and W. J. van de Berg (2011), A new albedo scheme for use in climate models over the Antarctic ice sheet, *J. Geophys. Res.*, *116*(D05114), doi:10.1029/2010JD015113.
- Marzeion, B., A. H. Jarosch, and M. Hofer (2012), Past and future sea-level change from the surface mass balance of glaciers, *The Cryosphere Discussions*, *6*(4), 3177–3241, doi:10.5194/tcd-6-3177-2012.
- Moss, R. H., et al. (2010), The next generation of scenarios for climate change research and assessment, *Nature*, *463*(7282), 747–756, doi:10.1038/nature08823.
- Radić, V., and R. Hock (2011), Regionally differentiated contribution of mountain glaciers and ice caps to future sea-level rise, *Nature Geosci.*, *4*, 91–94, doi:10.1038/ngeo1052.
- Rignot, E., I. Velicogna, M. R. van den Broeke, A. Monaghan, and J. T. M. Lenaerts (2011), Acceleration of the contribution of Greenland and Antarctic ice sheets to sea level rise, *Geophys. Res. Lett.*, *38*(L05503), doi:10.1029/2011GL046583.
- Sharp, M., D. O. Burgess, J. G. Cogley, M. Ecclestone, C. Labine, and G. J. Wolken (2011), Extreme melt on Canada's Arctic ice caps in the 21st century, *Geophys. Res. Lett.*, *38*(L11501), doi:10.1029/2011GL047381.
- Taylor, K. E., R. J. Stouffer, and G. A. Meehl (2007), A summary of the CMIP5 experiment design, *WORLD*, *4*, 1–33.
- The HadGEM2 Development Team (2011), The HadGEM2 family of Met Office Unified Model climate configurations, *Geosci. Model Dev.*, *4*(3), 723–757, doi:10.5194/gmd-4-723-2011.
- Uppala, S. M., et al. (2005), The ERA-40 re-analysis, *Quart. J. Roy. Meteor. Soc.*, *131*(612), 2961–3012, doi:10.1256/qj.04.176.
- Van Wychen, W., L. Copland, L. Gray, D. Burgess, B. Danielson, and M. Sharp (2012), Spatial and temporal variation of ice motion and ice flux from Devon Ice Cap, Nunavut, Canada, *J. Glaciol.*, *58*(210), 657–664, doi:10.3189/2012JoG11J164.
- Wouters, B., D. Chambers, and E. J. O. Schrama (2008), GRACE observes small-scale mass loss in Greenland, *Geophys. Res. Lett.*, *35*(20), 10.
- Zdanowicz, C., A. Smetny-Sowa, D. Fisher, N. Schaffer, L. Copland, J. Eley, and F. Dupont (2012), Summer melt rates on Penny Ice Cap, Baffin island: Past and recent trends and implications for regional climate, *J. Geophys. Res.*, *117*(F02006), doi:10.1029/2011JF002248.